Supplementary Information for

Global urban fractional changes at a 1km resolution throughout 2100 under eight SSP-RCP scenarios

Wanru He[1], Xuecao Li[1,2*], Yuyu Zhou[3*], Zitong Shi[4], Guojiang Yu[1], Tengyun Hu[5], Yixuan Wang[1], Jianxi Huang[1,2], Tiecheng Bai[6], Zhongchang Sun[7], Xiaoping Liu[8], Peng Gong[9]

[1] College of Land Science and Technology, China Agricultural University, Haidian, Beijing 100083, China

[2] Key Laboratory of Remote Sensing for Agri-Hazards, Ministry of Agriculture and Rural Affairs, Beijing 100083, China

[3] Department of Geological and Atmospheric Sciences, Iowa State University, Ames, IA 50011, USA

[4] National Institute of Natural Hazards, Ministry of Emergency Management of China, Beijing 100085, China

[5] Beijing Municipal Institute of City Planning and Design, Beijing 100045, China

[6] School of Information Engineering, Tarim University, Alaer 843300, China

[7] Key Laboratory of Digital Earth Science, Aerospace Information Research Institute (AIR), Chinese Academy of Sciences, Beijing 100101, China

[8] School of Geography and Planning, Sun Yat-Sen University, Guangzhou 510275, China

[9] Department of Geography, The University of Hong Kong, Hong Kong 999077, China

**Correspondence to*: Xuecao Li (xuecaoli@cau.edu.cn) and Yuyu Zhou (yuyuzhou@isatate.edu)

Supplementary texts

The Logistic-Trend-ISA-CA model is a self-evolution system, consisting of four primary components, including the suitability surface (here we implemented a logistic regression model for transition rules extraction, Eq. S1-2), the trend-adjusted neighborhood (Eq. 2-3), the stochastic perturbation (Eq. S3), and the land constraint.

We implemented a logistic regression model for transition rules extraction with considerations of various spatial proxies. The neighborhood configuration, which closely relates to its size, shape, and surrounding land cover types, is a basic and crucial component in the urban CA model as a driving force to modeling urban dynamics. Most urbanized pixels were developed following the historical pathway coupling with the neighborhood altering by the temporal trend. In this procedure, the non-urban grids are more likely to transform into urban grids in next iterations if there are more developed urban grids surrounded. Thereafter, the weighting factors of urban pixels developed in more recent years are higher than those developed in earlier years. We also included land constraint and stochastic perturbation in the developed Logistic-Trend-CA model. Land cover/use type in the initial year will influence spatial allocation in the urban sprawl process and restricted lands, such as water and protected areas, were not allowed for development in the Logistic-Trend-CA model; thereafter, they were represented as a land constraint term as Land = 0. Stochastic perturbation represents unconsidered factors (e.g., policies) in the modeling process.

$$z = b_0 + b_1 x_1 + \cdots + b_n x_n \tag{S1}$$

$$p_{suit} = \frac{\exp(z)}{1+\exp(z)} \tag{S2}$$

$$R_{ij}^{t} = 1 + (-\ln(\varphi))^{\alpha} \tag{S3}$$

where P_{suit} is the obtained suitability of development from the biophysical and socioeconomic conditions and b_i and x_i are the ith coefficient and spatial proxy, respectively. Ω is the influence of neighborhood considering the historical contexts of urban sprawl using a weighting factor of W_{ij}^{ts} (Eq. 2-3). R_{ij}^{t} is the stochastic perturbation, φ is a random value in [0, 1], and α is a parameter determining the degree of perturbation.

We then calculated the overall development probability based on the suitability surface, neighborhood, land constraint and stochastic perturbation. We determined their development probabilities P_{suit} using Eq. (4) based on urban time series data derived from Landsat. The units with the higher combined development probability have higher priority for urban grid allocation than those with lower probability.

Fig. S1

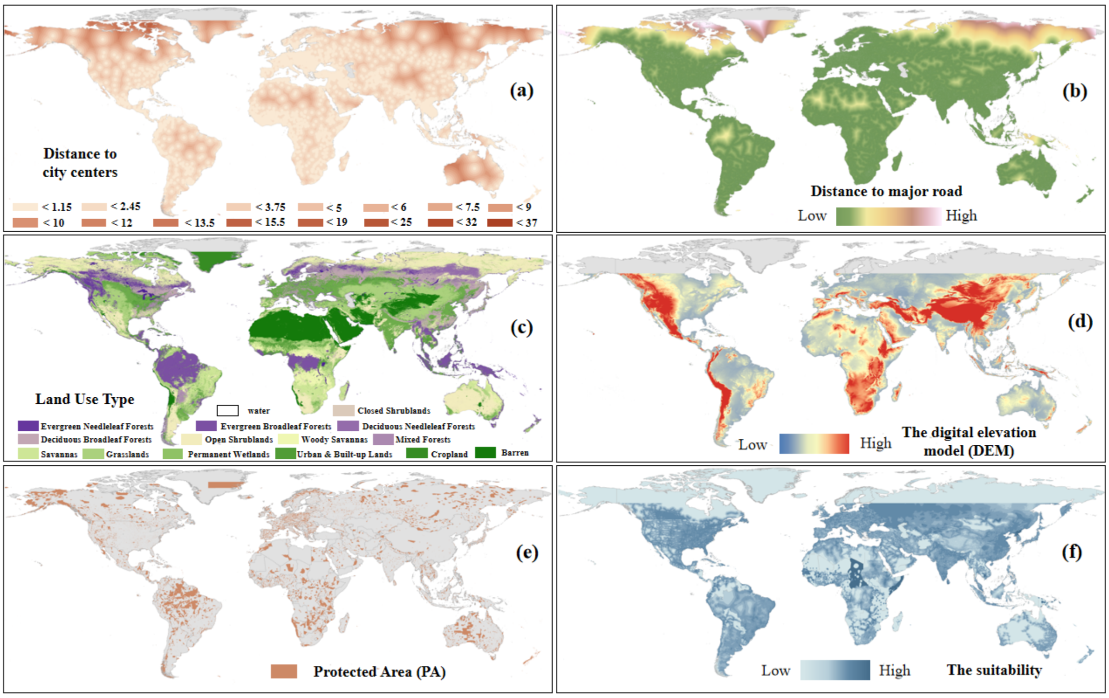

Fig S1. The distance to city centers (a), the distance to major road (b), the land use types (c), the digital elevation model (DEM) (d), the protected area (PA) (e), and the derived suitability surface at the global scale (f)

Fig. S2

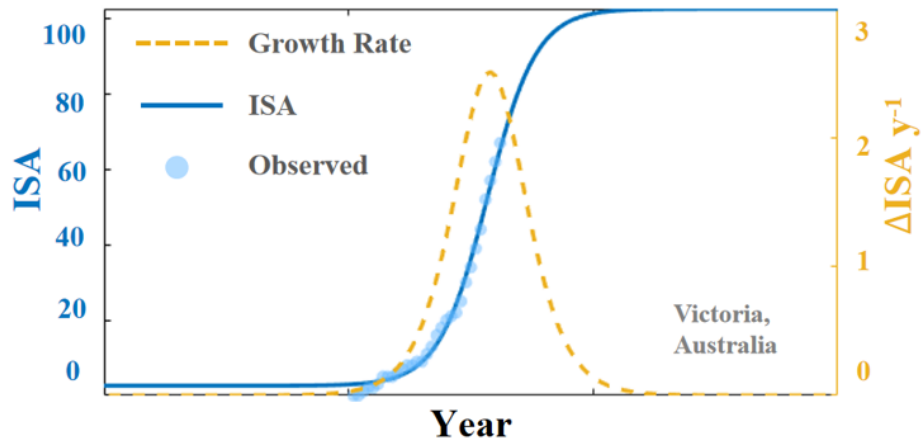

Fig S2. Illustration of the ISA-based urban area growth model in a specific region, with distinct ISA growth trends at different urbanization levels. Here we set the ISA conceptual model of Victoria in Australia as an example.

Fig. S3

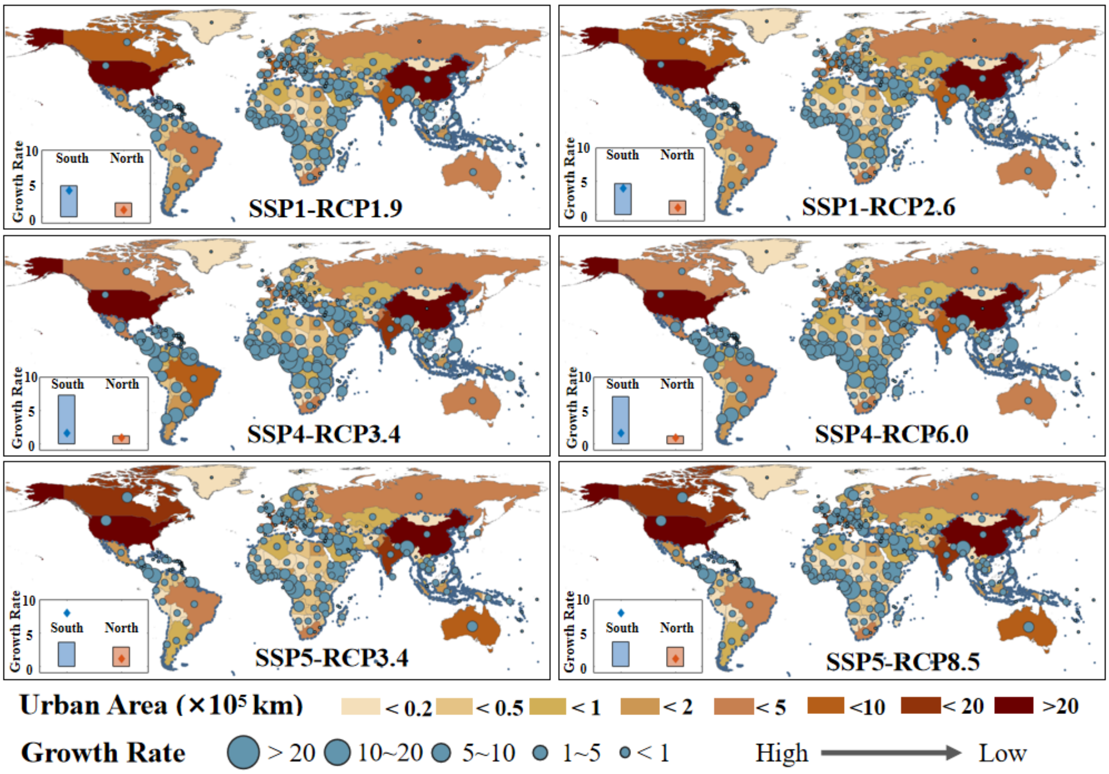

Fig S3. The average urban growth rate (2100/ 2015) derived from LUH2 at the country level, under various RCP levels and same SSP levels.

Fig. S4

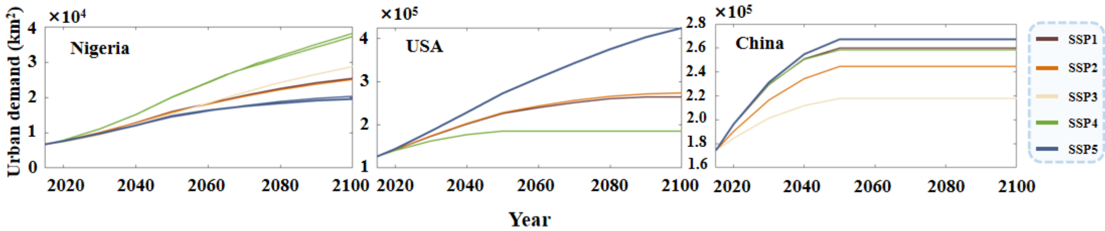

Fig S4. The future urban demand of the typical countries in Fig. 3.

Fig. S5

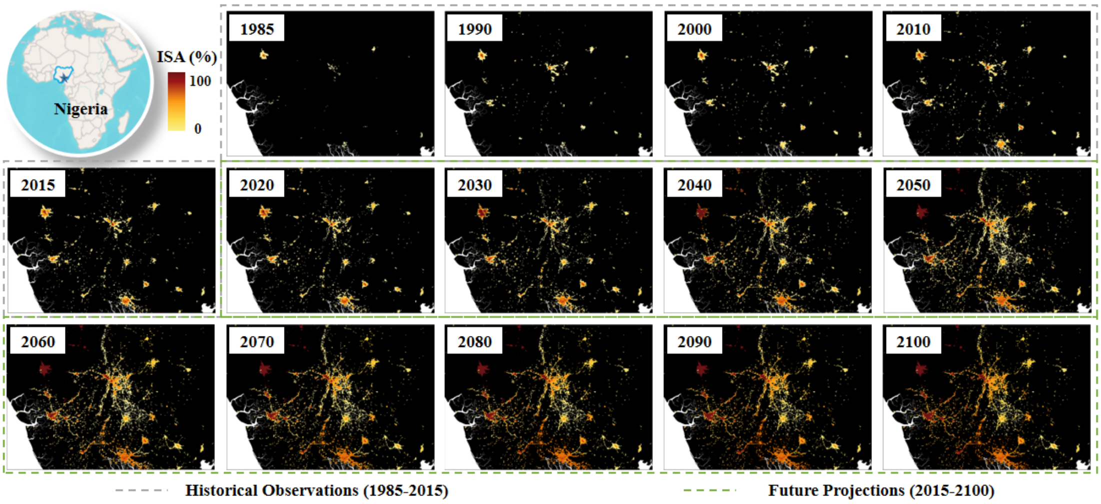

Fig S5. The temporal spatial patterns of urban sprawl of Nigeria at 1km spatial resolution from 1985 to 2100 under the most fluctuating scenario (SSP4-RCP6.0).

Fig. S6

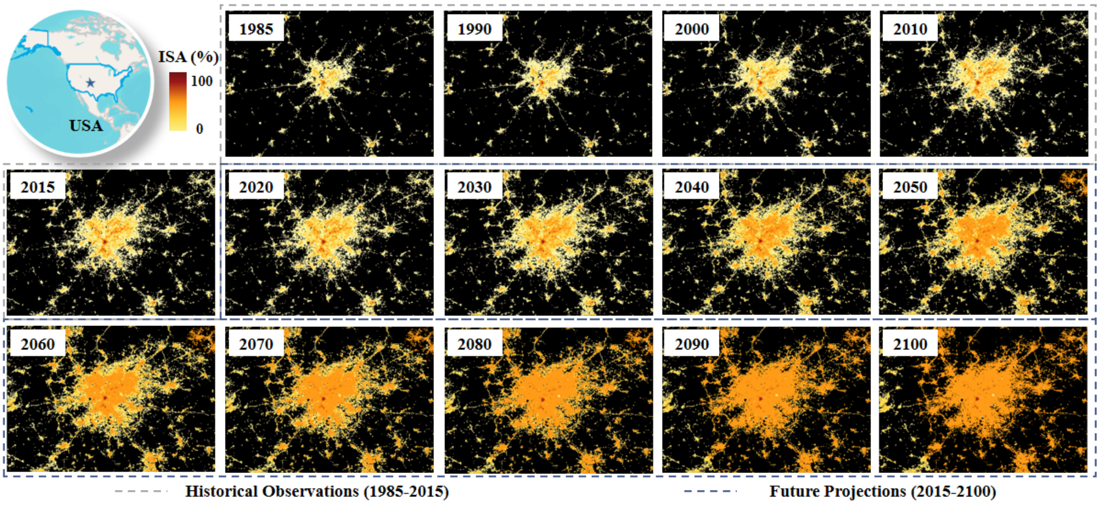

Fig S6. The temporal spatial patterns of urban sprawl of USA at 1km spatial resolution from 1985 to 2100 under the most fluctuating scenario (SSP5-RCP8.5).

Fig. S7

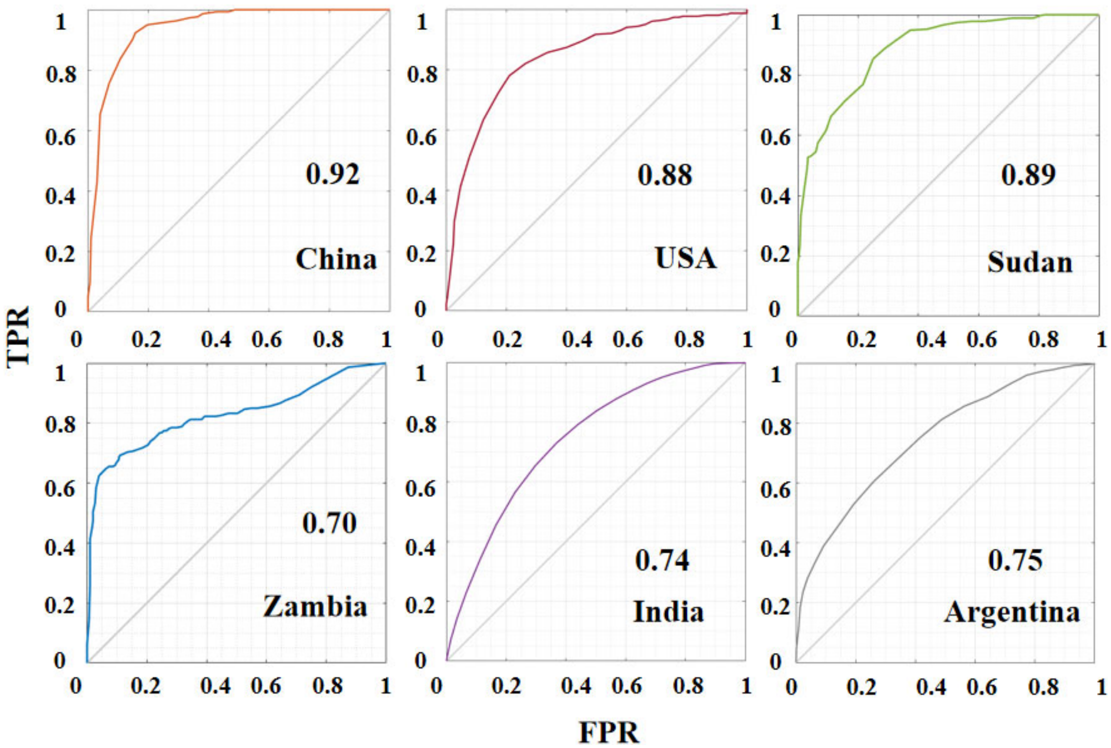

Fig S7. The ROC curves in some representative countries like China, USA, Sudan, Zambia, India, and Argentina.